Cell, Vol. 120, 701–713, March 11, 2005, Copyright ©2005 by Elsevier Inc. DOI 10.1016/j.cell.2005.01.015

Environmental Enrichment Reduces Aβ Levels and Amyloid Deposition in Transgenic Mice

Orly Lazarov,[1] John Robinson,[1] Ya-Ping Tang,[2] Ilana S. Hairston,[3] Zeljka Korade-Mirnics,[7] Virginia M.-Y. Lee,[4] Louis B. Hersh,[5] Robert M. Sapolsky,[3] Karoly Mirnics,[6,*] and Sangram S. Sisodia[1,*]

[1]Department of Neurobiology, Pharmacology, and Physiology and
[2]Department of Psychiatry
University of Chicago
Chicago, Illinois 60637
[3]Departments of Biological Sciences and of Neurology and Neurological Sciences
Stanford University
Stanford, California 94305
[4]Department of Pathology and Laboratory Medicine
Center for Neurodegenerative Disease Research
University of Pennsylvania School of Medicine
Philadelphia, Pennsylvania 19104
[5]Department of Molecular and Cellular Biochemistry
College of Medicine
University of Kentucky
Lexington, Kentucky 40536
[6]Department of Psychiatry
Department of Neurobiology
[7]Department of Pediatrics
University of Pittsburgh
Pittsburgh, Pennsylvania 15261

Summary

Cerebral deposition of β-amyloid (Aβ) peptides is an invariant pathological hallmark in brains of patients with Alzheimer's disease (AD) and transgenic mice coexpressing familial AD-linked APP and PS1 variants. We now report that exposure of transgenic mice to an "enriched environment" results in pronounced reductions in cerebral Aβ levels and amyloid deposits, compared to animals raised under "standard housing" conditions. The enzymatic activity of an Aβ-degrading endopeptidase, neprilysin, is elevated in the brains of "enriched" mice and inversely correlated with amyloid burden. Moreover, DNA microarray analysis revealed selective upregulation in levels of transcripts encoded by genes associated with learning and memory, vasculogenesis, neurogenesis, cell survival pathways, Aβ sequestration, and prostaglandin synthesis. These studies provide evidence that environmental enrichment leads to reductions in steady-state levels of cerebral Aβ peptides and amyloid deposition and selective upregulation in levels of specific transcripts in brains of transgenic mice.

Introduction

Alzheimer's disease (AD), the major cause of adult-onset dementia, is associated with progressive memory loss and severe cognitive decline. These clinical features are associated with deposition of β-amyloid (Aβ) peptides and neuronal loss in the cerebral cortex and hippocampal formation. Aβ peptides are liberated from the larger transmembrane amyloid precursor protein (APP) by the action of BACE 1 and γ-secretase. Early-onset, familial forms of the disease (FAD) are caused by expression of mutant variants of APP, presenilin 1 (PS1) or presenilin 2 (PS2) (Price and Sisodia, 1998). Expression of these mutant genes leads to the overproduction of highly fibrillogenic $A\beta_{42}$ peptides, and coexpression of FAD-linked PS1 and APP leads to accelerated amyloid deposition in the hippocampus and cerebral cortices of transgenic mice (Price and Sisodia, 1998).

In view of compelling evidence that has emerged to suggest that the brain, and the hippocampus and cortex in particular, exhibit environment-induced plasticity throughout adult life, and the demonstration that APP processing and Aβ production can be modulated by synaptic activity (Kamenetz et al., 2003; Nitsch et al., 1993), we tested the hypothesis that Aβ amyloidogenesis could be modulated by environmental "experience." The classical paradigm that has been employed to assess environment-induced plasticity is termed "environmental enrichment" and involves placing animals in large cages that contain running wheels, colorful tunnels, and assorted toys. Indeed, it is well established that animals placed in such environments exhibit enhanced memory function (Fordyce and Wehner, 1993), increased survival of newborn cells in the dentate gyrus (Kempermann et al., 1997), and enhanced recovery from lesion-induced memory deficits (Rampon et al., 2000). Morphologically, exposure to environmental enrichment is manifested in an increase in numbers of dendritic spines, extent of branching, and number of synapses per neuron (for review, see van Praag et al. [2000]), implying that neural outcomes are a function of the degree and nature of environmental experience.

We employed a well-established mouse model in which coexpression of familial AD (FAD)-linked APP "Swedish" (APPswe) and PS1ΔE9 polypeptide variants leads to Aβ deposition throughout the hippocampus and cortex (Lazarov et al., 2002). A cohort of newly weaned, male APPswe X PS1ΔE9 mice were exposed to an enriched environment conditions for 5 months, after which time the brains of these animals were examined using biochemical and histological approaches. We now show that environmental enrichment leads to marked reductions in both the steady-state levels of Aβ peptides and Aβ deposition in brains of enriched mice compared to mice in standard housing conditions. In parallel, we observe a significant elevation in the activity of an Aβ-degrading protease, neprilysin (NEP) in brain extracts from enriched mice compared to standard-housed animals. Using high-density Affymetrix GeneChips microarray technologies, we show that, in hippocampi of younger mice, the majority of transcripts that were significantly upregulated in enriched mice corresponded to immediate early genes (IEG), but tran-

*Correspondence: ssisodia@drugs.bsd.uchicago.edu (S.S.S.); karoly+@pitt.edu (K.M.)

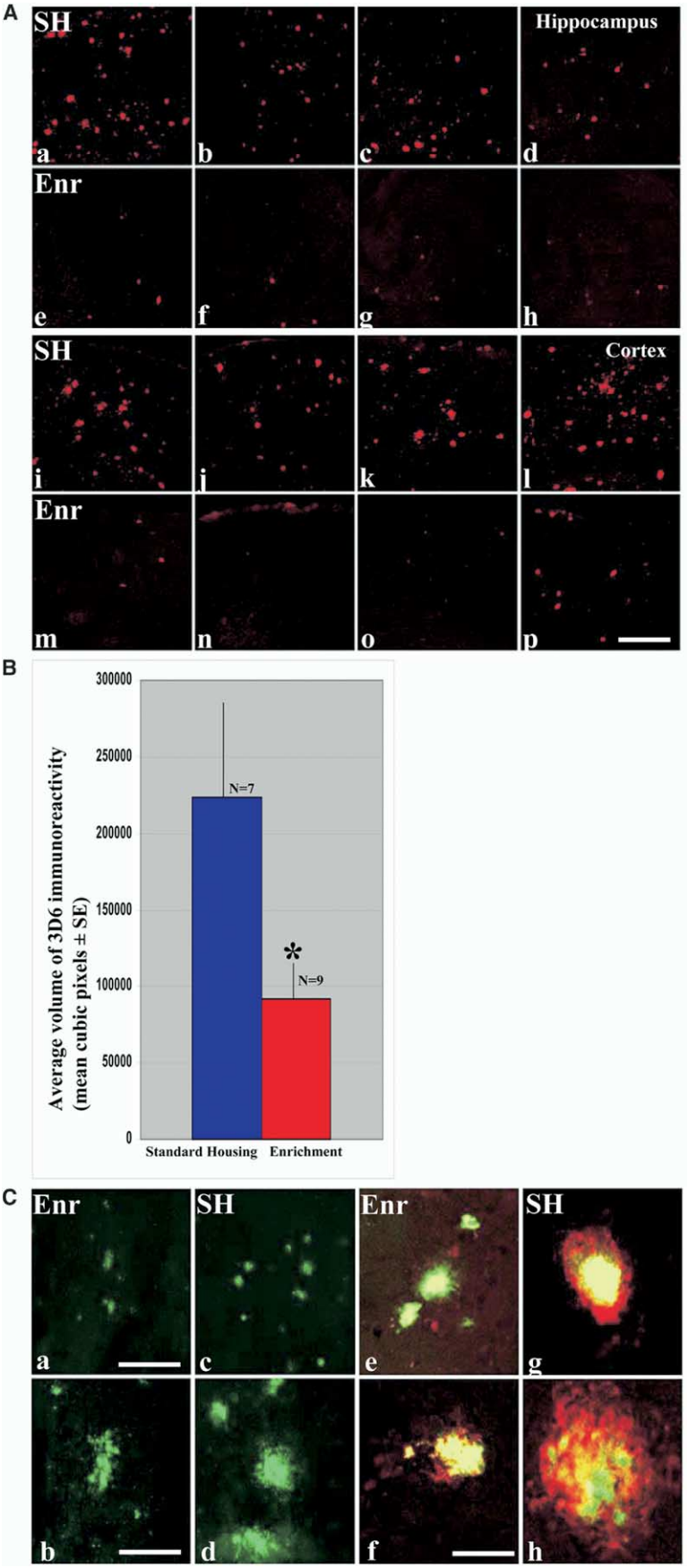

Figure 1. Reduced Amyloid Deposition in the Hippocampus and Cortex of Enriched versus Standard Housing Mice

(A) Immunohistochemical analysis of brain sections of standard housing (SH, [Aa]–[Ad], hippocampus; [Ai]–[Al], cortex) and enriched mice (Enr, [Ae]–[Ah], hippocampus; [Am]–[Ap], cortex) immunolabeled with anti-Aβ 3D6 antibodies. Pictures were taken from four enriched and four standard housing mice. Scale bar, 250 μm.

(B) Quantitative analysis of volume of amyloid burden in brains of standard housing and enriched mice. Volume is in arbitrary units (mean cubic pixels ± SE, ANOVA, $p \leq 0.0374$).

(C) Reduced number and size of thioflavine S-stained amyloid deposits in the hippocampus and cortex of enriched versus standard housing mice. Thioflavine S-positive amyloid deposits in brain sections of enriched (Enr; Ca, Cb, Ce, and Cf) and standard housing mice (SH; Cc, Cd, Cg, Ch). Size and abundance of thioflavine-positive structures in enriched (a = low power; b = high power) is reduced compared to standard housing mice (c = low power; d = high power). For (Ca) and (Cc), scale bar, 250 μm. For (Cb) and (Cd), scale bar, 120 μm. Double labeling with thioflavine S and anti-Aβ 3D6 antibodies reveals overlap staining at the core of the amyloid deposits, while the periphery of the deposit is stained mostly with anti-Aβ 3D6 antibodies (Cg and Ch). In contrast, the vast majority of amyloid deposits in brain sections of enriched mice had little 3D6-positive peripheral staining (Ce and Cf). Scale bar, 60 μm.

A

Enrichment	Enriched High activity	Enriched Low activity
% time running	44.3-62.4	<10.9
% time climbing	<0.5	<1
% time resting	<0.1	3.6-33.6

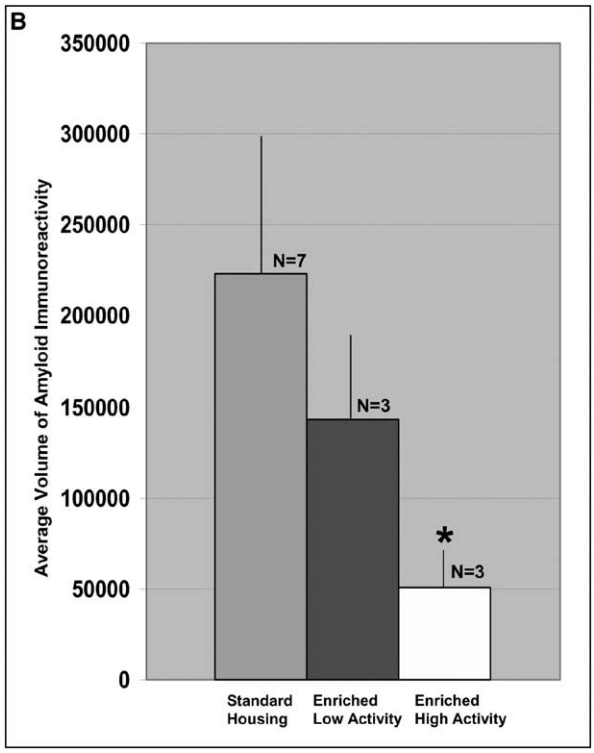

Figure 2. Amyloid Deposition as a Function of Activity Level

(A) Activity level of mice during exposure to enriched environment. Activity level of the mice was observed and recorded periodically. The time spent by the mice for each activity group is expressed as a percentage of total observation time.

(B) Amyloid deposition in the brain of enriched mice as a function of their activity level. Amyloid deposition in the brains of enriched mice was detected and analyzed as described above (see Figures 1A and 1B). Levels of amyloid deposition were found to be inversely correlated with the activity level of the mice (mean ± SE; ANOVA, $p \leq 0.0116$).

scripts encoding polypeptides involved in Aβ sequestration, endothelial function, and phospholipid metabolism were also elevated. This study provides evidence that steady-state levels of cerebral Aβ peptides and amyloid deposition can be modulated by environmental factors.

Results

Environmental Enrichment Leads to Reduced Aβ Deposition

At 1 month of age, an experimental group of nine male APPswe X PS1ΔE9 mice were exposed to enriched environment conditions for 5 months. During the last month, we documented the behavior and activity of a subset of these animals in the "enrichment" cage. Seven male mice at the age of 1 month were maintained in standard housing conditions for 5 months, and these served as the control group. Animals were euthanized and brain sections were probed with 3D6 antibodies, specific for an epitope at or near the amino terminus of Aβ (Kim et al., 2001). Bound antibodies were detected by fluorescently labeled secondary antibodies and visualized by confocal microscopy. We observed a dramatic reduction in amyloid deposition in the cortex and hippocampus of enriched mice compared to standard housing counterparts (Figure 1A). Morphometric analysis of 3D6-immunoreactive brain sections confirmed that enriched mice exhibited significantly less amyloid burden in the hippocampus and cortex compared to standard housing mice (Figure 1B). Thioflavine S staining revealed a reduced abundance and size of deposits with fibrillar Aβ in enriched mice (Figures 1Ca and 1Cb) compared to standard housing mice (Figures 1Cc and 1Cd). Co-staining of brain sections with thioflavine S and 3D6 antibodies revealed overlap in staining at the core of the amyloid deposits in sections from either enriched or standard mice (compare Figures 1Ce and 1Cf to 1Cg and 1Ch, respectively). However, 3D6 immunoreactivity in the plaque periphery in enriched mice was reduced compared to standard housing mice (compare Figures 1Ce and 1Cf to 1Cg and 1Ch, respectively).

To examine a possible correlation between the extent of amyloid deposition and activity of the mice in the enriched environment, we documented the behavior of six enriched mice during the last month prior to sacrifice. Some mice were highly active, spending more than 40% of their enrichment time running on the running wheels, while others had low activity (Figure 2A). Remarkably, enriched mice exhibiting high activity levels showed the most significant reductions in amyloid burden (Figure 2B). Thus, at least in this small cohort of animals, exercise appears to play a significant role in modulating amyloid deposition.

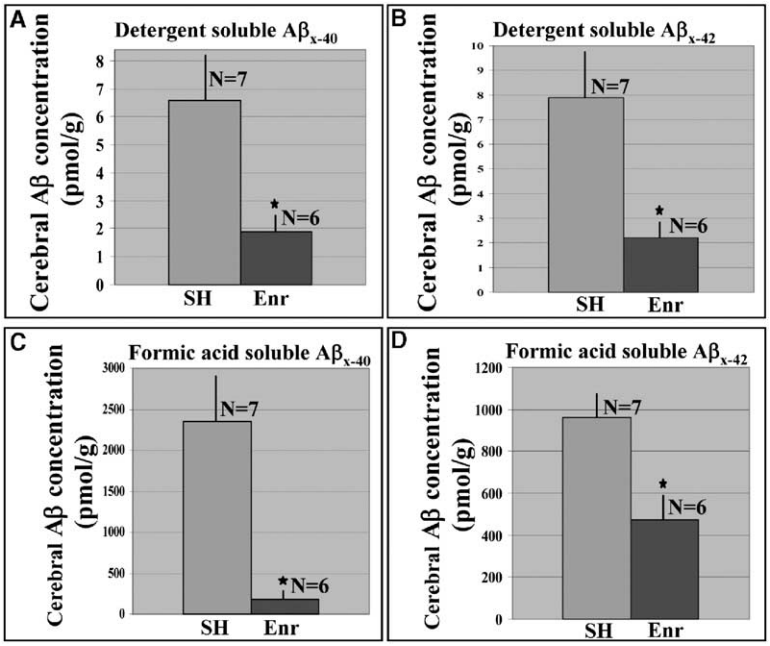

Figure 3. Reduced Steady-State Levels of Cerebral Aβ in the Brains of Enriched Mice

Cerebral steady state levels of $A\beta_{x-40/42}$ were quantified by sandwich ELISA (Suzuki et al., 1994). Levels of $A\beta_{x-40}$ and $A\beta_{x-42}$ were significantly reduced in both detergent-soluble (A and B) and formic acid-soluble (C and D) brain extracts of enriched mice (Enr) compared to standard housing (SH) mice (mean ± SE, ANOVA; for (A), $p \leq 0.0287$; for (B), $p \leq 0.02228$; for (C), $p \leq 0.0404$; for (D), $p \leq 0.0010$).

Reduction of Aβ Levels in Brains of Enriched Mice

We considered the possibility that reduced Aβ deposition in brains of enriched mice is due to lower steady-state levels of Aβ itself. To examine this issue, we prepared detergent and formic acid extracts of hemibrains from seven standard housing animals and six enriched mice and quantified Aβ levels in these samples. In agreement with the morphometric studies, sandwich ELISA analyses revealed that levels of detergent- (Figures 3A and 3B) and formic acid-soluble (Figures 3C and 3D) $A\beta_{x-40}$ (Figures 3A and 3C) and $A\beta_{x-42}$ (Figure 3B and 3D) peptides were significantly reduced in the brains of the enriched mice compared to standard housing mice. The marked reduction of detergent-insoluble, formic acid-extractable $A\beta_{x-40}$ and $A\beta_{x-42}$ peptides in brain extracts of the enriched mice agrees with our earlier observations of reduced numbers and size of thioflavine S-positive deposits in brain sections of enriched mice.

To assess whether alterations in APP processing might account for the reduction in Aβ levels, we subjected detergent-soluble extracts to Western blot analysis to examine the steady-state levels of APP, soluble APP derivatives (sAPP), membrane-tethered APP carboxyl-terminal derivatives (APP-CTF), and Aβ peptides. We noted slight variations in levels of full-length APP in brain extracts prepared from both standard housing and enriched groups, but these were fully consistent with the variations observed with a protein-loading control, α-tubulin (see Figures S1Aa and S1Ad, respectively, in the Supplemental Data available with this article online; quantification in Figure S1Ba). Similarly, differences in levels of APP-CTFs levels between samples parallel the variation in full-length APP or α-tubulin (Figure S1Ab; quantification in Figures S1Bb and S1Bd). In contrast, the levels of detergent-extractable Aβ peptides in brains of most of the enriched mice samples were considerably lower than those from standard housing mice. (Figures S1Ac and S1Ad, compare lanes 10–16 with lanes 5–9, respectively). Considerable differences were observed in levels of detergent-extractable Aβ peptides detected by Aβ N-terminal-specific antibody 3D6 (see Figure S1Ac) or an end-specific antibody, 2G3, that detects the carboxyl-terminus of Aβ1–40, 11–40, or 17–40 (DeMattos et al., 2001; Figure S1Ad). Most notably, the last three samples in the enriched group (Figures S1Ac and S1Ad, lanes 16–18) were animals with the highest amyloid burden. Densitometric quantification of the immunoblots revealed that the levels of total Aβ and $A\beta_{11/40}$ were significantly reduced in extracts from brains of enriched mice compared to standard housing mice (Figures S1Bc and S1Bf for Aβ and Figure S1Bd for $A\beta_{x-40}$), findings that support the sandwich ELISA assays. These results suggest that, while the enrichment protocol has little discernable impact on APP processing in the CNS, this procedure has a profound impact on the steady-state levels of Aβ peptides.

Elevated Activity of Neprilysin, an Aβ-Degrading Protease

Our finding that cerebral levels of soluble $A\beta_{x-40}$ were reduced in brains of enriched mice suggested that there might be an increase in the activity of an Aβ-degrading protease. Taken together with our finding that insoluble, highly fibrillogenic $A\beta_{x-42}$ peptides were reduced further suggested that an Aβ clearance and/or degradation mechanism(s) might be enhanced. We first considered the possibility that the activity of Aβ-degrading proteases might have been upregulated in the brains of mice exposed to enriched environment. To test this proposal, we examined the enzymatic activity of two proteases implicated in Aβ degradation in vitro and in vivo: neprilysin (NEP), ~97 kDa membrane bound zinc metal-

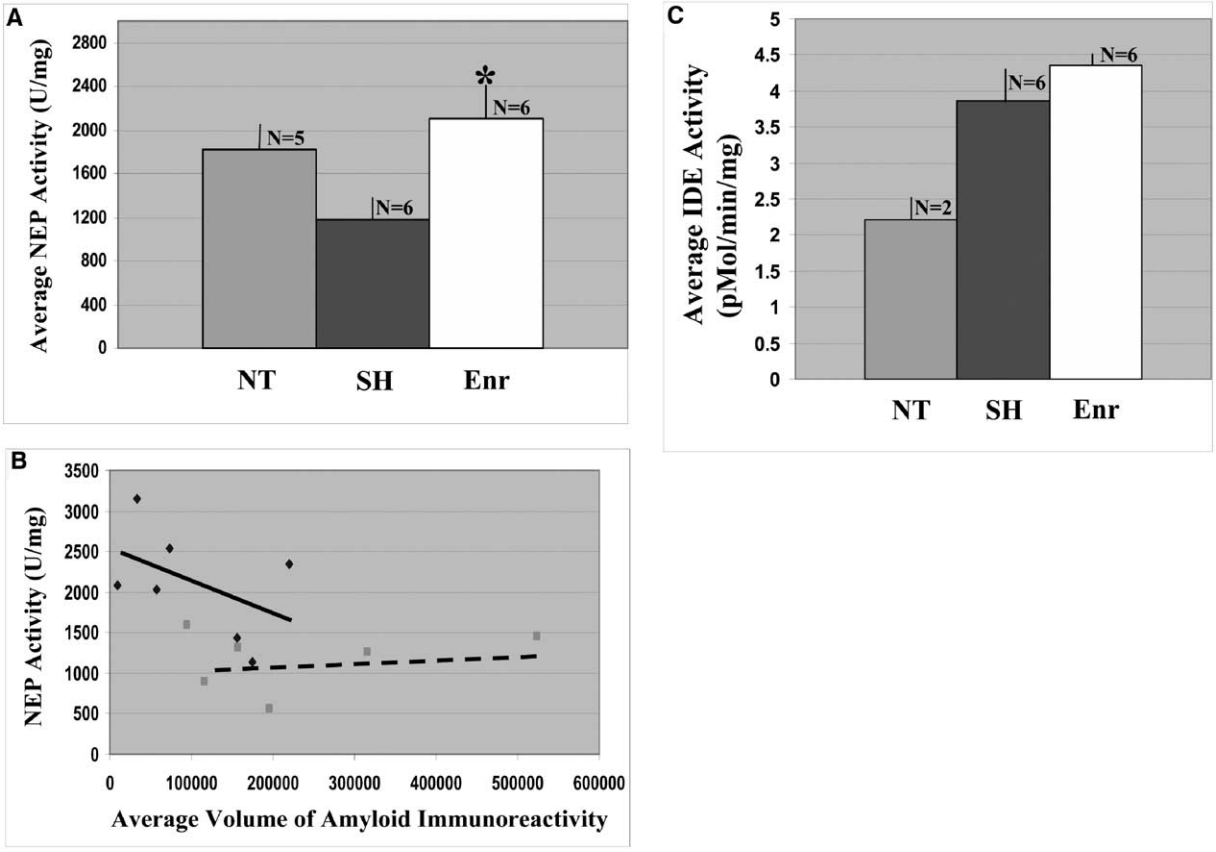

Figure 4. Elevated Neprilysin Activity in Brains of Enriched Mice

(A) Average NEP activity in the brain of nontransgenic (NT), enriched (Enr), and standard housing (SH) mice (mean ± SE; ANOVA, $p \leq 0.0128$). NEP activity is increased in brains of mice that were exposed to enriched conditions, compared to mice kept in standard housing conditions.

(B) NEP activity as a function of amyloid deposition. An inverse relation is observed between amyloid burden and NEP activity in brains of enriched mice (standard housing, dashed line; enrichment, solid line).

(C) Activity level of IDE in brains of enriched and standard housing mice (mean ± SE). Differences between IDE activity levels in brains of enriched and standard housing mice were found to be nonsignificant.

loendopeptidase (Turner et al., 2001); and insulysin (insulin-degrading enzyme; IDE), an ~110 kDa thiol zinc metalloendopeptidase (Farris et al., 2003; Miller et al., 2003). We first examined NEP activity in brains of 6-month-old nontransgenic mice compared to 6-month-old standard housing mice (Figure 4A) and found that there was slight reduction in NEP activity in brain extracts of the transgenic animals (Figure 4A). We considered the possibility that the reduction in neprilysin activity in the brains of transgenic animals with amyloid deposition might be the result of competition from high levels of endogenous Aβ in the assay preparation. To examine this issue, we measured NEP activity in brain extracts from three 6-month-old nontransgenic mice "spiked" with up to 2000 pmols/gm purified $A\beta_{40}$. These studies failed to reveal any inhibitory effect of purified Aβ on endogenous NEP activity (data not shown). While there is no clear explanation for the observed difference in NEP activity between nontransgenic and standard housed mice, the observation is consistent with the finding that, in AD brain, neprilysin is reduced ~50% relative to controls in regions of high plaque content but is unchanged in brain areas with moderate or low plaque burden (Yasojima et al., 2001a; Yasojima et al., 2001b). In any event, the most striking finding of this study is that NEP activity was significantly elevated in brain extracts from enriched mice compared to standard housed animals (Figure 4A). Moreover, NEP activity was inversely related to amyloid deposition in the brains of enriched mice (Figure 4B). In contrast, IDE activity in extracts from brains of enriched and standard housing mice were quite similar (Figure 4C). We interpret our studies to suggest that reductions in Aβ levels in enriched mice might, at least in part, be the consequence of elevated NEP activity.

Elevated Expression of Immediate Early Genes in Brains of Enriched Mice

Although elevated NEP activity in brains of enriched mice might contribute to the lowering of Aβ levels and Aβ deposition, it was equally conceivable that additional mechanisms might be operative that influence aspects of Aβ production and/or deposition. In order to develop an unbiased understanding of gene expression changes that occur in brains of enriched mice, we employed a two-step microarray analysis strategy of a co-

Table 1. Differentially Expressed Genes between Enriched and Standard Housing Mice across Two Cohorts

Probe Set	Gene	Accession	LocusLink	ALR E1R1	ALR E1R2	Pval E1	ALR E2	Pval E2	*ALR comb*[a]	*Pval comb*
1423100_at	FBJ osteosarcoma oncogene	AV026617	14281	1.47	1.60	0.00003	1.68	0.00001	1.61	0.00000
1418687_at	Activity regulated cytoskeletal-associated protein	NM_018790	11838	1.09	1.35	0.00010	1.44	0.00003	1.33	0.00000
1417065_at	Early growth response 1	NM_007913	13653	1.07	1.22	0.00075	1.00	0.00211	1.07	0.00002
1448830_at	Dual specificity phosphatase 1	NM_013642	19252	0.81	1.22	0.00000	0.89	0.00016	0.95	0.00000
1415899_at	Jun-B oncogene	NM_008416	16477	0.77	0.79	0.00023	1.02	0.00071	0.90	0.00000
1416505_at	Nuclear receptor subfamily 4, group A, member 1	NM_010444	15370	0.70	0.86	0.00014	0.87	0.00008	0.82	0.00000
1427683_at	Early growth response 2	X06746	13654	0.56	0.50	0.00027	0.93	0.00054	0.73	0.00000
1422134_at	FBJ osteosarcoma oncogene B	NM_008036	14282	0.46	0.40	0.01754	0.64	0.00186	0.54	0.00037
1415834_at	Dual specificity phosphatase 6	NM_026268	67603	0.35	0.69	0.03369	0.50	0.00806	0.51	0.00250
1449977_at	Early growth response 4	NM_020596	13656	0.40	0.55	0.00173	0.53	0.00731	0.50	0.00016
1416129_at	RIKEN cDNA 1300002F13 gene	NM_133753	74155	0.38	0.58	0.03723	0.50	0.00252	0.49	0.00097
1427351_s_at	Heavy chain of IgM	BB226392	16019	0.43	0.25	0.04288	0.53	0.00426	0.44	0.00175
1448306_at	NFkappa light chain gene enhancer, alpha	NM_010907	18035	0.28	0.68	0.00171	0.37	0.00805	0.43	0.00017
1448890_at	Kruppel-like factor 2	NM_008452	16598	0.54	0.37	0.01317	0.33	0.00017	0.39	0.00003
1449731_s_at	NFkappa light chain gene enhancer, alpha	AI462015	18035	0.21	0.39	0.00537	0.40	0.00459	0.35	0.00029
1416442_at	Immediate early response 2	NM_010499	15936	0.31	0.23	0.00842	0.38	0.00070	0.32	0.00008
1436893_a_at	axotrophin	BE288026	57438	−0.49	−0.25	0.01383	−0.38	0.00095	−0.38	0.00016

Seventeen genes showed differential expression across the two cohorts of biological replicates. E1R1, experiment 1, technical replicate 1; E1R2, experiment 1, technical replicate 2; E2, experiment 2 (biological replicate); ALR comb, average log ratio across the biological replicates; Pval comb, p value across the biological replicates. Note that 16 of 17 probe sets showed increased expression.

[a] Average log ratio (ALR) = 1 corresponds to a 2-fold change.

hort of APPswe X PS1ΔE9 mice that were exposed to environmental enrichment from the time of weaning for 2 months to a cohort of mice housed under standard conditions. The 3 month time point was chosen to uncover transcriptome changes that preceded amyloid deposition and to maximize the discovery of transcriptome changes that may be causally related to alterations in Aβ metabolism and the development of micropathology. This strategy also allowed us to avoid expression changes that are secondary to amyloid deposition in the brain tissue.

We first performed duplicate microarray analysis on hippocampal tissue from three enriched and four standard housing mice. Based on this data set, we defined an enrichment-dependent transcriptome profile. The validity of the determined profile, which also served as our hypothesis, was tested in a second microarray experiment on a new cohort of four enriched and four control mice at 3 months of age. Using this biological replicate data set validation strategy, 17 genes were identified as differentially expressed (Table 1) with a false discovery rate of <5.9% (Figure S2). Sixteen of the genes showed increased expression in the hippocampi of enriched animals, while a single gene transcript was underexpressed. The vast majority of these transcripts are encoded by immediate early genes (IEGs) that control early transcriptional activation. Two-way hierarchical clustering in Genes@Work (Califano et al., 2000) for the 17 genes correctly classified the samples according to enrichment phenotype in both of the technical and biological replicate experiments (Figure 5A).

In addition to the validation strategy across the two cohorts of animals, we performed a direct groupwise comparison of the seven enriched and eight control animals. In addition to the same 17 genes identified with our first comparison strategy, we found 24 more probe sets that showed a highly significant ($p < 0.01$ and ALR > |0.263|) change across the enriched and control animals (Table 2) (Seo et al., 2004) with an estimated FDR of 5.5% (Figure S3). These results showed also a high concordance with a secondary Significance Analysis of Microarrays (SAM) examination. Of the total of 41 probe sets, 13 were redundant and encoded six of the same genes. Interestingly, the enriched animals reported more frequent and more robust (36/41 probe sets; mean ALR = 0.55) overexpression of genes than downregulation of transcripts (5/41 probe sets; mean ALR = −0.31). Two-way clustering of the expression data of these 41 probe sets also separated the enriched and control animals according to their correct phenotypes (Figure 5B). Again, the vast majority of genes showing expression change were related to early transcriptome activation, and these genes encoded polypeptides involved in a variety of processes associated with learning and memory, vasculogenesis, neurogenesis, and cell survival pathways (see Discussion).

In addition to the latter "data-driven" analysis approach, we also performed a "knowledge-based" ex-

ploration of our data set. Namely, the levels of transcripts encoding transthyretin (TTR), prostaglandin D2 synthase (PDGS2), insulin-like growth factor 2 (IGF2), insulin-like growth factor 2 binding protein (IGFBP2), and ectonucleotide pyrophosphatase (ENP2) have been shown to be elevated in the Tg2576 transgenic mouse that overexpresses APPswe and at a time point well before the onset of Aβ deposition (Stein and Johnson, 2002). Stein and Johnson (2002) suggested that the expression of these latter genes, involved in Aβ sequestration (TTR) and cell survival pathways (IGF-2, IGFBP2), were responsible for the lack of neurodegeneration in the Tg2576 mouse model. When we examined the expression level of these transcripts across the cohort of enriched animals and standard housed controls, we found considerable individual variability between animals in both the control and experimental groups (data not shown). To uncover potentially significant data that is lost in the individual variability of the animals, we decided to focus our attention on mice that all originated from the same parents (five in the enriched group, two in standard housing controls) (Figure S4). Comparison of the microarray data for these mice revealed a remarkable upregulation of TTR and PDGS2 in the animals that were subject to environmental enrichment. Three independent probes reported an 11.2- to 44.3-fold increase in TTR transcripts (one-tailed $p < 0.05$; Figures S4A and S4B). Furthermore, two independent PDGS2 probes reported a 2.1- to 2.3-fold upregulation in the experimental mice ($p = 0.002$; Figure S4C). In addition, two probes of ENP2 reported a 1.6- to 5.1-fold increase in the enriched mice ($p = 0.017$ and $p = 0.084$, respectively; Figure S4D). Finally, both IGF2 and IGFBP2 reported modestly increased mean expression levels that did not reach statistical significance ($p = 0.155$ and $p = 0.076$, respectively; Figures S4E and S4F, respectively). Importantly, the expression levels of TTR, PDGS2, and ENP2 were highly correlated between these mice (TTR-PDGS2, $r = 0.76$; TTR-ENP2, $r = 0.93$; PDGS2-ENP2, $r = 0.87$), suggesting that these genes may be part of a coregulated transcript network.

Discussion

We have employed transgenic mice that overexpress FAD-linked APP and PS1 transgenes to test the hypothesis that activity would modulate APP and Aβ metabolism in vivo. We chose to address this issue using an experimental paradigm termed environmental enrichment, a procedure shown to significantly improve memory function associated with profound morphological changes in synaptic and dendritic architecture as well as enhanced vascular plasticity and neurogenesis (for review, see Churchill et al. [2002]). This experimental paradigm has allowed us to offer several critical insights that may have a profound significant impact on developing strategies for the prevention of Alzheimer's disease.

First, we show that exposure of male transgenic mice to an enriched environment from the time of weaning until the age of 6 months results in a marked reduction in Aβ deposition in the CNS compared to mice held in standard housing conditions. Remarkably, the reduction in Aβ burden in this cohort of enriched mice is inversely correlated with physical activity, as defined as the time spent on the running wheel. In this regard, evidence has accrued to suggest that exercising and physical training may impede aging-related processes (for review, see Mattson [2000] and Mattson et al. [2001]), induce structural changes and recovery from memory deficits and brain lesions (Rampon et al., 2000), and ameliorate cognitive function in older adults and AD patients (for review, see Kramer et al. [2002]). While the inverse correlation between running and amyloid deposition is provocative, it will be necessary to evaluate the phenomenon in larger cohorts of animals and to isolate exercise from the other visual, social, and spatial stimuli in the enriched environment before arriving at definitive conclusions about the unique role of physical activity in modulating Aβ deposition. Second, we demonstrate that steady-state levels of soluble and formic acid-soluble Aβ peptides are reduced in brains of enriched mice compared to standard housing mice. Western blot analyses revealed that enrichment does not profoundly alter APP processing but alters the levels of accumulated Aβ peptides.

It is important to note that, in contrast to our findings, Jankowsky and colleagues recently reported that environmental enrichment enhances amyloid deposition and steady-state Aβ levels in a different mouse strain that coexpresses APPswe and PS1ΔE9 (Jankowsky et al., 2003). However, we note several critical differences in the experimental approaches: first, subjects in the report of Jankowsky et al. (2003) were females, in contrast to the males used in the present report; in this regard, there is a clear but poorly understood enhancement of amyloid burden in females compared to age-matched males (Wang et al., 2003). Second, there was a 2:1 ratio of mice to running wheels in our study, in contrast to the 8:1 ratio in the report by Jankowsky et al. (2003); the latter setting was likely to generate hierarchical competition and stress for access to wheels, potentially blunting the salutary effects of enrichment. Finally, subjects culled from the enrichment colony at various points in the Jankowsky study (Jankowsky et al., 2003) were replaced with new individuals; such group reorganization is a well-characterized model for inducing sustained social stress (Blanchard et al., 2003; Sapolsky, 1993), again potentially off-setting the effects of enrichment.

Third, we show that the activity of an Aβ-degrading protease, neprilysin, is elevated in brains of enriched mice compared to nontransgenic mice or mice raised in standard housing conditions. These data are consistent with several in vivo studies showing that ectopic overexpression of NEP in brains of transgenic mice leads to reduced Aβ deposition and clearance of preexisting Aβ deposits (Iwata et al., 2004; Marr et al., 2003).

Fourth, we employed high-density oligonucleotide arrays to an unbiased assessment of gene expression changes that occur in brains of enriched mice compared to standard housed animals. Direct groupwise comparison of seven enriched and eight control animals revealed a total of 41 probe sets that showed a highly significant change across the enriched and control animals, with 13 of these probe sets being redun-

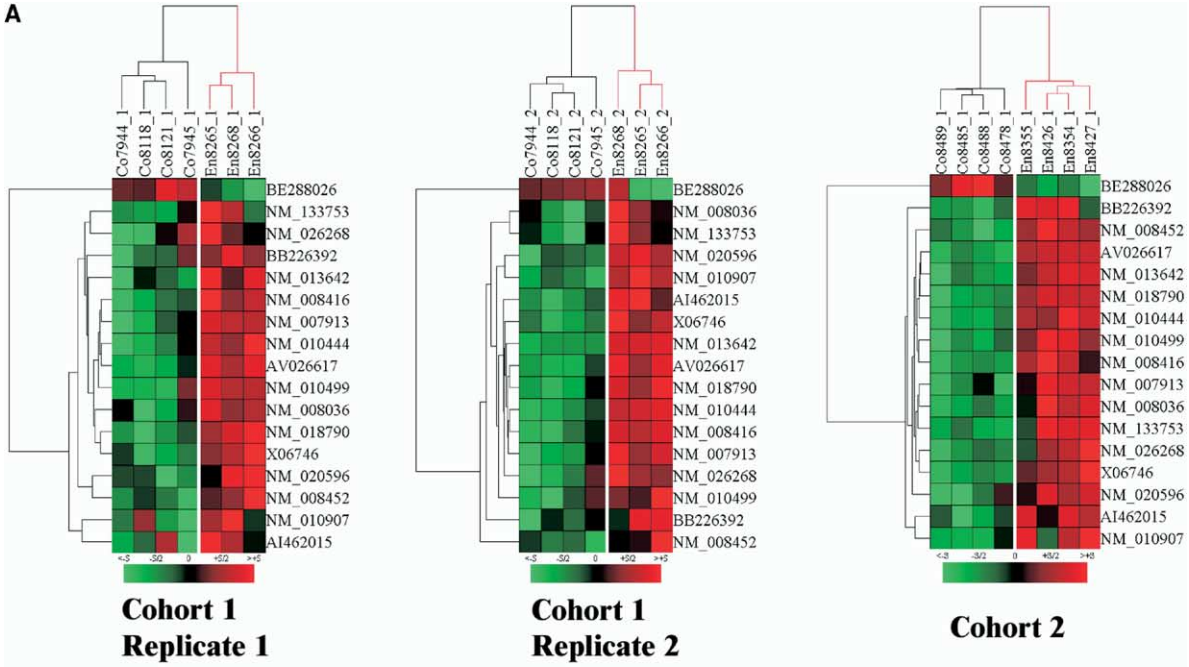
A
Co7944_1
Co8118_1
Co8121_1
Co7945_1
En8265_1
En8268_1
En8266_1
BE288026
NM_133753
NM_026268
BB226392
NM_013642
NM_008416
NM_007913
NM_010444
AV026617
NM_010499
NM_008036
NM_018790
X06746
NM_020596
NM_008452
NM_010907
AI462015
<-S -S/2 0 +S/2 >+S
Cohort 1
Replicate 1
Co7944_2
Co8118_2
Co8121_2
Co7945_2
En8268_2
En8265_2
En8266_2
BE288026
NM_008036
NM_133753
NM_020596
NM_010907
AI462015
X06746
NM_013642
AV026617
NM_018790
NM_010444
NM_008416
NM_007913
NM_026268
NM_010499
BB226392
NM_008452
<-S -S/2 0 +S/2 >+S
Cohort 1
Replicate 2
Co8489_1
Co8485_1
Co8488_1
Co8478_1
En8355_1
En8426_1
En8354_1
En8427_1
BE288026
BB226392
NM_008452
AV026617
NM_013642
NM_018790
NM_010444
NM_010499
NM_008416
NM_007913
NM_008036
NM_133753
NM_026268
X06746
NM_020596
AI462015
NM_010907
<-S -S/2 0 +S/2 >+S
Cohort 2

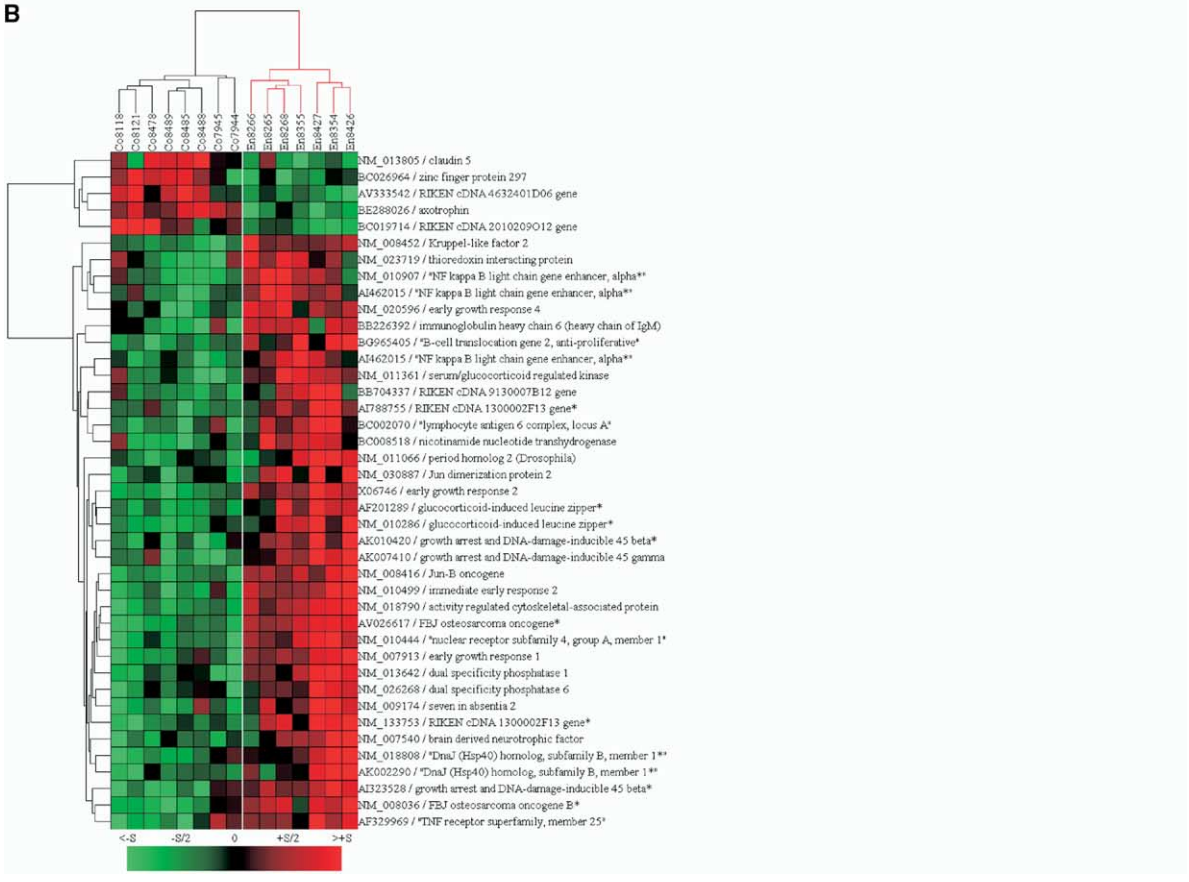
B
Co8118
Co8121
Co8478
Co8489
Co8485
Co8488
Co7945
Co7944
En8266
En8265
En8268
En8355
En8427
En8354
En8426
NM_013805 / claudin 5
BC026964 / zinc finger protein 297
AV333542 / RIKEN cDNA 4632401D06 gene
BE288026 / axotrophin
BC019714 / RIKEN cDNA 2010209O12 gene
NM_008452 / Kruppel-like factor 2
NM_023719 / thioredoxin interacting protein
NM_010907 / *NF kappa B light chain gene enhancer, alpha**
AI462015 / *NF kappa B light chain gene enhancer, alpha**
NM_020596 / early growth response 4
BB226392 / immunoglobulin heavy chain 6 (heavy chain of IgM)
BG965405 / *B-cell translocation gene 2, anti-proliferative*
AI462015 / *NF kappa B light chain gene enhancer, alpha**
NM_011361 / serum/glucocorticoid regulated kinase
BB704337 / RIKEN cDNA 9130007B12 gene
AI788755 / RIKEN cDNA 1300002F13 gene*
BC002070 / *lymphocyte antigen 6 complex, locus A*
BC008518 / nicotinamide nucleotide transhydrogenase
NM_011066 / period homolog 2 (Drosophila)
NM_030887 / Jun dimerization protein 2
X06746 / early growth response 2
AF201289 / glucocorticoid-induced leucine zipper*
NM_010286 / glucocorticoid-induced leucine zipper*
AK010420 / growth arrest and DNA-damage-inducible 45 beta*
AK007410 / growth arrest and DNA-damage-inducible 45 gamma
NM_008416 / Jun-B oncogene
NM_010499 / immediate early response 2
NM_018790 / activity regulated cytoskeletal-associated protein
AV026617 / FBJ osteosarcoma oncogene*
NM_010444 / *nuclear receptor subfamily 4, group A, member 1*
NM_007913 / early growth response 1
NM_013642 / dual specificity phosphatase 1
NM_026268 / dual specificity phosphatase 6
NM_009174 / seven in absentia 2
NM_133753 / RIKEN cDNA 1300002F13 gene*
NM_007540 / brain derived neurotrophic factor
NM_018808 / *DnaJ (Hsp40) homolog, subfamily B, member 1**
AK002290 / *DnaJ (Hsp40) homolog, subfamily B, member 1**
AI323528 / growth arrest and DNA-damage-inducible 45 beta*
NM_008036 / FBJ osteosarcoma oncogene B*
AF329969 / *TNF receptor superfamily, member 25*
<-S -S/2 0 +S/2 >+S

dant. The vast majority of genes showing elevated expression encode polypeptides involved in a variety of processes associated with learning and memory, vasculogenesis, neurogenesis, and cell survival pathways. Consistent with earlier studies that exercise induces angiogenesis in the CNS following environmental enrichment (Black et al., 1990; Isaacs et al., 1992; Swain et al., 2003), we observed elevated expression of mRNA encoding EGR-1 (or NGF-1A, Zif268), a zinc finger transcription factor that is rapidly induced by a variety of stimuli, including growth factors, cytokines, and hypoxia, and plays a critical role in the expression of downstream genes that regulate angiogenesis (Abe and Sato, 2001; Mechtcheriakova et al., 1999; Silverman and Collins, 1999). In this regard, transcripts encoding a transcriptional regulator of endothelial cell activation, termed Kruppel-like factor (KLF2) (SenBanerjee et al., 2004), are also elevated in the hippocampi of enriched mice.

Transcripts encoding brain-derived neurotrophic factor (BDNF), implicated in long-term synaptic plasticity in the adult hippocampus, are significantly upregulated in brains of our enriched mice and have long been known to be elevated in animals following exercise (Farmer et al., 2004; Tong et al., 2001). Similarly, the enrichment-dependent upregulation of serum and glucocorticoid-inducible protein kinase (SGK) in the hippocampus of our enriched mice has been shown to be elevated in hippocampus of environmentally enriched rats (Lee et al., 2003) and correlates with memory consolidation in spatial learning paradigms (Tsai et al., 2002). We also observed marked elevations in levels of transcripts associated with neurogenesis, known to occur in the dentate gyrus as a consequence of environmental enrichment (Kempermann et al., 1997; Kempermann et al., 1998; van Praag et al., 1999). For example, expression of mRNA encoding B cell translocation gene 2 (Btg2) has been shown to be induced in vivo during neurogenesis (Iacopetti et al., 1999) and is transiently upregulated during differentiation of NGF-treated PC12 cells (el-Ghissassi et al., 2002).

What is the functional significance of the upregulation of the immediate early genes (IEGs) and other factors involved in memory retrieval and consolidation in the enriched APPswe X PS1ΔE9 mice? We have not performed any physiological or behavioral analyses of standard housing versus enriched mice, and further behavioral studies in this direction are clearly warranted. However, the expression of several IEGs, including Arc, Nur77, and Zif268, are markedly downregulated in brains of mice that coexpress mutant APP and PS1 transgenes at a time when these mice exhibit cognitive dysfunction (Dickey et al., 2003; Dickey et al., 2004). On the other hand, we now show that the levels of these IEGs were significantly upregulated in the hippocampus of enriched mice compared to mice kept in standard housing conditions. We suggest that the microarray results in enriched mice might be predictive of improvements in cognition in these animals, but additional studies will be necessary to examine this issue. In this regard, a recent study by Arendash and colleagues (Arendash et al., 2004) revealed that exposure of older APPswe mice to an enriched environment lead to global, overall improvement in cognitive function across several behavioral tasks that was not associated with a change in brain Aβ deposition.

In addition to upregulated expression of transcripts encoded by the IEGs, we also identified a set of transcripts shown previously to be elevated in brains of APPswe transgenic mice prior to the onset of Aβ deposition. These transcripts, encoding transthyretin (TTR), prostaglandin D2 synthase (PDGS2), insulin-like growth factor 2 (IGF2), insulin-like growth factor 2 binding protein (IGFBP2), and ectonucleotide pyrophosphatase (ENP2), have been argued to be neuroprotective (Stein and Johnson, 2002). The elevation in TTR levels in APPswe mice at an early age (Stein and Johnson, 2002) and in enriched mice may lead to sequestration of soluble Aβ peptides and, ultimately, their toxicity. PDGS2 is expressed at very high levels in the choroids plexus and exhibits high-affinity binding to lipophilic molecules (Urade and Hayaishi, 2000), leading us to speculate that Aβ might also be bound by this polypeptide. Ectonucleotide phosphohydrolase (CD39), expressed in microglia, endothelial cells, and smooth muscles of the cerebral vasculature (Braun et al., 2000), is induced by hypoxia and appears to modulate endothelial barrier function in this setting (Eltzschig et al., 2003; Pinsky et al., 2002).

In summary, we provide the first experimental evidence that exposure to environmental enrichment markedly reduces Aβ levels and amyloid deposition in brains of transgenic mice and that the effects may, at least in part, be mediated by alterations in Aβ catabolism or Aβ sequestration. Finally, the demonstration that enrichment enhances expression of genes known to regulate vasculogenesis offers the provocative suggestion that modifications of the blood-brain barrier and associated factors may have a profound impact on Aβ clearance

Figure 5. Hierarchical Clustering of Gene Probe Sets

(A) Two-way hierarchical clustering of 17 gene probe sets identified in Table 1. Gene probes are represented by rows with corresponding GenBank accession numbers, and columns represent experimental animals (red, enriched; black lines, controls). RMA-standardized log2 intensity values are clustered based on Euclidian distance. Colored squares represent increased (red) or decreased expression (green) for a single gene in a single animal. Color brightness is proportional to the magnitude of expression difference. Left and middle panels represent two independent technical replicates originating from the same mice. Right panel corresponds to a biological replicate on a new cohort of animals. Note that the experimental animals correctly cluster according to their genotype in all panels. Furthermore, the enriched animals report increased expression for 16 of 17 genes.

(B) Two-way hierarchical clustering of 41 gene probe sets identified in Table 2. Figure layout similar to that described in Figure 5A. These genes included all the 17 gene probe sets showing differential expression identified in Figure 5A and Table 1. For six genes, multiple probe sets obtained identical results. Of the 41 probe sets, only five reported decreased expression.

Table 2. Differentially Expressed Genes between Seven Enriched and Eight Standard Housing Mice

Probe Set	Gene Name	Symbol	Accession	LocusLink	ALR[b]	pVal	SAM dval	SAM Rank
1423100_at	FBJ osteosarcoma oncogene	Fos	AV026617	14281	1.64	0.00000	−7.41	−1
1418687_at	Activity regulated cytoskeletal-associated protein	Arc	NM_018790	11838	1.36	0.00000	−6.49	−2
1417065_at	Early growth response 1	Egr1	NM_007913	13653	1.10	0.00009	−4.17	−6
1448830_at	Dual specificity phosphatase 1	Dusp1	NM_013642	19252	0.99	0.00019	−3.81	−7
1415899_at	Jun-B oncogene	Junb	NM_008416	16477	0.92	0.00000	−4.94	−3
1416505_at	Nuclear receptor subfamily 4, group A, member 1	Nr4a1	NM_010444	15370	0.85	0.00001	−4.47	−4
1416041_at	Serum/glucocorticoid regulated kinase	Sgk	NM_011361	20393	0.75	0.00055	−3.24	−9
1427683_at	Early growth response 2	Egr2	X06746	13654	0.74	0.00001	−4.36	−5
1425281_a_at	Glucocorticoid-induced leucine zipper[a]	Gilz	AF201289	14605	0.64	0.00023	−3.29	−8
1415834_at	Dual specificity phosphatase 6	Dusp6	NM_026268	67603	0.54	0.00403	−2.43	−22
1422134_at	FBJ osteosarcoma oncogene B	Fosb	NM_008036	14282	0.54	0.00014	−3.19	−10
1416755_at	DnaJ (Hsp40) homolog, subfamily B, member 1[a]	Dnajb1	NM_018808	81489	0.52	0.00224	−2.55	−18
1416129_at	RIKEN cDNA 1300002F13 gene[a]	na	NM_133753	74155	0.50	0.00035	−2.92	−11
1420772_a_at	Glucocorticoid-induced leucine zipper[a]	Gilz	NM_010286	14605	0.49	0.00058	−2.80	−15
1449977_at	Early growth response 4	Egr4	NM_020596	13656	0.49	0.00064	−2.77	−16
1416250_at	B cell translocation gene 2, anti-proliferative	Btg2	BG965405	12227	0.49	0.00041	−2.86	−13
1449262_s_at	RIKEN cDNA 9130007B12 gene	na	BB704337	108852	0.48	0.00462	−2.32	−23
1449773_s_at	Growth arrest and DNA-damage-inducible 45 beta[a]	Gadd45b	AI323528	17873	0.48	0.00030	−2.90	−12
1417185_at	Lymphocyte antigen 6 complex, locus A	Ly6a	BC002070	110454	0.46	0.00192	−2.48	−20
1416756_at	DnaJ (Hsp40) homolog, subfamily B, member 1[a]	Dnajb1	AK002290	81489	0.45	0.00492	−2.25	−26
1417602_at	Period homolog 2 (Drosophila)	Per2	NM_011066	18627	0.43	0.00828	−2.10	−30
1427351_s_at	Immunoglobulin heavy chain 6 (heavy chain of IgM)	Igh-6	BB226392	16019	0.43	0.00167	−2.45	−21
1448306_at	NF kappa B light chain gene enhancer, alpha[a]	Nfkbia	NM_010907	18035	0.41	0.00083	−2.53	−19
1448890_at	Kruppel-like factor 2	Klf2	NM_008452	16598	0.38	0.00028	−2.65	−17
1422168_a_at	Brain derived neurotrophic factor	BDNF	NM_007540	12064	0.38	0.00268	−2.24	−27
1416105_at	Nicotinamide nucleotide transhydrogenase	Nnt	BC008518	18115	0.35	0.00153	−2.26	−25
1449731_s_at	NF kappa B light chain gene enhancer, alpha[a]	Nfkbia	AI462015	18035	0.34	0.00178	−2.21	−28
1416442_at	Immediate early response 2	Ier2	NM_010499	15936	0.33	0.00002	−2.81	−14
1422231_a_at	TNF receptor superfamily, member 25	Tnfrsf25	AF329969	85030	0.32	0.00471	−2.00	−39
1419816_s_at	RIKEN cDNA 1300002F13 gene[a]	na	AI788755	74155	0.31	0.00337	−2.01	−35
1415996_at	Thioredoxin interacting protein	Txnip	NM_023719	56338	0.28	0.00795	−1.81	−46
1453851_a_at	Growth arrest and DNA-damage-inducible 45 gamma	Gadd45g	AK007410	23882	0.28	0.00024	−2.28	−24
1448170_at	Seven in absentia 2	Siah2	NM_009174	20439	0.27	0.00108	−2.07	−31
1450350_a_at	Jun dimerization protein 2	Jundm2	NM_030887	81703	0.27	0.00401	−1.89	−41
1450971_at	Growth arrest and DNA-damage-inducible 45 beta[a]	Gadd45b	AK010420	17873	0.27	0.00079	−2.10	−29
1420088_at	NF kappa B light chain gene enhancer, alpha[a]	Nfkbia	AI462015	18035	0.26	0.00136	−2.00	−37
1452170_at	RIKEN cDNA 2010209012 gene	na	BC019714	100910	−0.29	0.00152	2.08	3
1448705_at	Zinc finger protein 297	Zfp297	BC026964	81630	−0.29	0.00826	1.82	6
1437746_at	RIKEN cDNA 4632401D06 gene	na	AV333542	74342	−0.30	0.00067	2.23	2
1417839_at	Claudin 5	Cldn5	NM_013805	12741	−0.31	0.00729	1.87	5
1436893_a_at	Axotrophin	Axot	BE288026	57438	−0.38	0.00002	3.00	1

Forty-one genes showed differential expression across the whole data set. Table layout similar to that in Table 1, with the addition of the last two columns, which represent significance analysis of microarrays d values and rank. Thirty-six of 41 changed probe sets reported expression increases in the enriched environment-maintained animals. The outcome of the two analytical methods almost identical—all of the 36 genes with decreased expression in the Student's t-test ranked in the top 46 decreased genes by SAM, and the five most increased genes we found ranked in the top six by SAM.

[a] More than one probe set obtained convergent results.

[b] ALR of 1 = 2-fold change.

(DeMattos et al., 2002a; DeMattos et al., 2002b; Ji et al., 2001; Shibata et al., 2000).

Experimental Procedures

Transgenic Mice

Mice coexpressing FAD mutant human PS1ΔE9 and a chimeric mouse-human APP_{695} harboring a human Aβ domain and mutations (K595N, M596L) linked to Swedish FAD pedigrees (APPswe) have been described previously (Lazarov et al., 2002). Background strains include APPswe [C3H/HeJ × C57BL/6J F3] × C57BL/6J n1; PS1ΔE9 C3H/HeJ × C57BL/6J F3. Mice were screened for the blindness-causing retinal degeneration *rd* mutation and found to be wild-type (data not shown).

Enrichment Setting

Animal experiments were conducted in accordance with institutional and NIH guidelines. Male offspring of transgenic breeding pairs APPswe × PS1ΔE9 were separated from their mother at 3 weeks of age (after weaning), genotyped, and housed four males to a cage. Enriched environment was composed of large cages (3.236×10^4 cm^3), running wheels, colored tunnels, toys, and chewable material. For 1 month, mice were exposed to enriched environment every day for 3 hr and were returned to their original cages for the remaining 21 hr. After 1 month of daily enrichment, mice were introduced to the enriched environment three times a week for an additional 4 months. Mice were sacrificed at age of 6 months. Following weaning, a control group of animals was maintained for 5 months in standard housing conditions.

Tissue Processing and Immunohistochemistry

Brains were isolated, and the hemispheres were separated and frozen on dry ice. The right hemisphere was kept intact for immunohistochemistry. The left hemisphere was cut longitudinally into three segments; the medial segment was used for examination of protein expression by Western blot analysis (see below), the central segment for analyzing NEP and IDE activity (see below), and the lateral segment for Aβ quantification by ELISA (see below). The right hemisphere was cryosectioned horizontally into 20 μm sections, and sections were mounted on gelatin-coated slides. Sections were kept in −20°C until use. Immunostaining of sections, confocal imaging, and quantification of amyloid deposition were performed as previously described (Lazarov et al. [2002] or see Supplemental Experimental Procedures). Thioflavine S staining was performed as previously described (Benzing et al., 1993).

Extraction of Brain Proteins for Western Blot Analysis

Brains were homogenized in extraction buffer (50 mM Tris [pH 7.2], 150 mM NaCl, 5 mM EDTA, protease inhibitor mixture [Sigma], and 100 mM PMSF) using ground glass microhomogenizers. Following addition of 1% SDS, the homogenate was centrifuged for 10 min at 10,000 × g. Protein concentration of the supernatant fraction was determined using BCA-protein assay (Pierce), and equal amounts of proteins were analyzed by Western blot. Brain extracts were subject to Tris-Glycine or Tris-Tricine SDS-PAGE. Proteins were detected by Western blot analysis.

Antibodies

For Western blotting or immunohistochemistry, the following antibodies were used as previously described: CT15 (Sisodia et al., 1993), mAb22C11 (Hilbich et al., 1993; Weidemann et al., 1989), mouse anti-α-tubulin (Sigma 1:1,000,000), anti-Aβ mAb3D6 (1:2,500, [Kim et al., 2001]), anti-$Aβ_{40}$ mAb2G3 (1:2,500), Cy5- or Cy3-conjugated donkey anti-mouse IgG (1:250).

Sandwich ELISA Analysis

Cerebral Aβ was detected using ELISA protocols described previously (Suzuki et al., 1994; Turner et al., 1996). To detect detergent-soluble cerebral Aβ, brains were homogenized in RIPA buffer containing protease inhibitors. Extracts were sonicated and spun at 100,000 × g for 20 min at 4°C. Insoluble pellets were further extracted in 70% formic acid by sonication and spun at 100,000 × g for 20 min. Samples were neutralized in 1 M Tris buffer and diluted in blocking buffer before loading on ELISA. Aβ was captured with either JRF/cA$β_{40/10}$ or JRF/cA$β_{42/26}$, monoclonal antibodies specific for $Aβ_{40}$ and $Aβ_{42}$, respectively, supplied by Dr. M. Mercken (Janssen Research Foundation, Beerse, Belgium). Captured peptides were reported with horseradish peroxidase-conjugated m266, a monoclonal antibody recognizing residues 13–28 of Aβ (Seubert et al., 1992).

NEP and IDE Activity Assay

Each brain was homogenized for 5 s in 1 ml of 50 mM potassium phosphate buffer pH 7.3 containing 200 μM PMSF and 5 μ/ml aprotinin. The samples were centrifuged at 1000 × g for 20 min at 4°C and the supernatant fraction centrifuged again at 100,000 × g for 10 min. The 100,000 × g supernatant fraction was used for IDE activity measurements, while the pellet was resuspended in 200 μl of 20-mM MES (pH 6.5) containing 200 μM PMSF and 5 μg/ml aprotinin and used for neprilysin activity measurements.

IDE activity was measured by following the release of trichloroacetic acid soluble peptides from iodinated insulin (Song et al., 2003). Neprilysin activity was measured by following the cleavage of glutyl-Ala-Ala-Phe-2-methoxy-4-napthylamide (Sigma) using a coupled fluorescent assay (Li and Hersh, 1995).

Microarray Experiments

See Supplemental Experimental Procedures for a detailed description of microarray procedure and analyses.

Supplemental Data

Supplemental Data include four figures and Supplemental Experimental Procedures and can be found with this article online at http://www.cell.com/cgi/content/full/120/5/701/DC1/.

Acknowledgments

This study was supported by NIH AG021494 (S.S.S.) and the Ellison Medical Research Foundation (S.S.S.); AG11542 (V.M.-Y.L.); and NIDA (DA02243), NIA (AG19323), and the Alzheimer's Association (L.B.H.). The authors thank the Adler Foundation (I.S.H. and R.M.S.). The authors thank Dr. Angele Parent for help with statistics. The authors are thankful to Travis Unger, Dominique Arion, and Kathie C. Douglass for superb technical assistance with the microarray experiments.

Received: August 20, 2004
Revised: November 17, 2004
Accepted: January 13, 2005
Published: March 10, 2005

References

Abe, M., and Sato, Y. (2001). cDNA microarray analysis of the gene expression profile of VEGF-activated human umbilical vein endothelial cells. Angiogenesis *4*, 289–298.

Arendash, G.W., Garcia, M.F., Costa, D.A., Cracchiolo, J.R., Wefes, I.M., and Potter, H. (2004). Environmental enrichment improves cognition in aged Alzheimer's transgenic mice despite stable beta-amyloid deposition. Neuroreport *15*, 1751–1754.

Benzing, W.C., Mufson, E.J., and Armstrong, D.M. (1993). Immunocytochemical distribution of peptidergic and cholinergic fibers in the human amygdala: their depletion in Alzheimer's disease and morphologic alteration in non-demented elderly with numerous senile plaques. Brain Res. *625*, 125–138.

Black, J.E., Isaacs, K.R., Anderson, B.J., Alcantara, A.A., and Greenough, W.T. (1990). Learning causes synaptogenesis, whereas motor activity causes angiogenesis, in cerebellar cortex of adult rats. Proc. Natl. Acad. Sci. USA *87*, 5568–5572.

Blanchard, R.J., Wall, P.M., and Blanchard, D.C. (2003). Problems in the study of rodent aggression. Horm. Behav. *44*, 161–170.

Braun, N., Sevigny, J., Robson, S.C., Enjyoji, K., Guckelberger, O., Hammer, K., Di Virgilio, F., and Zimmermann, H. (2000). Assignment

of ecto-nucleoside triphosphate diphosphohydrolase-1/cd39 expression to microglia and vasculature of the brain. Eur. J. Neurosci. *12*, 4357–4366.

Califano, A., Stolovitzky, G., and Tu, Y. (2000). Analysis of gene expression microarrays for phenotype classification. Proc. Int. Conf. Intell. Syst. Mol. Biol. *8*, 75–85.

Churchill, J.D., Galvez, R., Colcombe, S., Swain, R.A., Kramer, A.F., and Greenough, W.T. (2002). Exercise, experience and the aging brain. Neurobiol. Aging *23*, 941–955.

DeMattos, R.B., Bales, K.R., Cummins, D.J., Dodart, J.C., Paul, S.M., and Holtzman, D.M. (2001). Peripheral anti-A beta antibody alters CNS and plasma A beta clearance and decreases brain A beta burden in a mouse model of Alzheimer's disease. Proc. Natl. Acad. Sci. USA *98*, 8850–8855.

DeMattos, R.B., Bales, K.R., Cummins, D.J., Paul, S.M., and Holtzman, D.M. (2002a). Brain to plasma amyloid-beta efflux: a measure of brain amyloid burden in a mouse model of Alzheimer's disease. Science *295*, 2264–2267.

DeMattos, R.B., Bales, K.R., Parsadanian, M., O'Dell, M.A., Foss, E.M., Paul, S.M., and Holtzman, D.M. (2002b). Plaque-associated disruption of CSF and plasma amyloid-beta (Abeta) equilibrium in a mouse model of Alzheimer's disease. J. Neurochem. *81*, 229–236.

Dickey, C.A., Loring, J.F., Montgomery, J., Gordon, M.N., Eastman, P.S., and Morgan, D. (2003). Selectively reduced expression of synaptic plasticity-related genes in amyloid precursor protein + presenilin-1 transgenic mice. J. Neurosci. *23*, 5219–5226.

Dickey, C.A., Gordon, M.N., Mason, J.E., Wilson, N.J., Diamond, D.M., Guzowski, J.F., and Morgan, D. (2004). Amyloid suppresses induction of genes critical for memory consolidation in APP + PS1 transgenic mice. J. Neurochem. *88*, 434–442.

el-Ghissassi, F., Valsesia-Wittmann, S., Falette, N., Duriez, C., Walden, P.D., and Puisieux, A. (2002). BTG2(TIS21/PC3) induces neuronal differentiation and prevents apoptosis of terminally differentiated PC12 cells. Oncogene *21*, 6772–6778.

Eltzschig, H.K., Ibla, J.C., Furuta, G.T., Leonard, M.O., Jacobson, K.A., Enjyoji, K., Robson, S.C., and Colgan, S.P. (2003). Coordinated adenine nucleotide phosphohydrolysis and nucleoside signaling in posthypoxic endothelium: role of ectonucleotidases and adenosine A2B receptors. J. Exp. Med. *198*, 783–796.

Farmer, J., Zhao, X., van Praag, H., Wodtke, K., Gage, F.H., and Christie, B.R. (2004). Effects of voluntary exercise on synaptic plasticity and gene expression in the dentate gyrus of adult male Sprague-Dawley rats in vivo. Neuroscience *124*, 71–79.

Farris, W., Mansourian, S., Chang, Y., Lindsley, L., Eckman, E.A., Frosch, M.P., Eckman, C.B., Tanzi, R.E., Selkoe, D.J., and Guenette, S. (2003). Insulin-degrading enzyme regulates the levels of insulin, amyloid beta-protein, and the beta-amyloid precursor protein intracellular domain in vivo. Proc. Natl. Acad. Sci. USA *100*, 4162–4167.

Fordyce, D.E., and Wehner, J.M. (1993). Physical activity enhances spatial learning performance with an associated alteration in hippocampal protein kinase C activity in C57BL/6 and DBA/2 mice. Brain Res. *619*, 111–119.

Hilbich, C., Monning, U., Grund, C., Masters, C.L., and Beyreuther, K. (1993). Amyloid-like properties of peptides flanking the epitope of amyloid precursor protein-specific monoclonal antibody 22C11. J. Biol. Chem. *268*, 26571–26577.

Iacopetti, P., Michelini, M., Stuckmann, I., Oback, B., Aaku-Saraste, E., and Huttner, W.B. (1999). Expression of the antiproliferative gene TIS21 at the onset of neurogenesis identifies single neuroepithelial cells that switch from proliferative to neuron-generating division. Proc. Natl. Acad. Sci. USA *96*, 4639–4644.

Isaacs, K.R., Anderson, B.J., Alcantara, A.A., Black, J.E., and Greenough, W.T. (1992). Exercise and the brain: angiogenesis in the adult rat cerebellum after vigorous physical activity and motor skill learning. J. Cereb. Blood Flow Metab. *12*, 110–119.

Iwata, N., Mizukami, H., Shirotani, K., Takaki, Y., Muramatsu, S., Lu, B., Gerard, N.P., Gerard, C., Ozawa, K., and Saido, T.C. (2004). Presynaptic localization of neprilysin contributes to efficient clearance of amyloid-beta peptide in mouse brain. J. Neurosci. *24*, 991–998.

Jankowsky, J.L., Xu, G., Fromholt, D., Gonzales, V., and Borchelt, D.R. (2003). Environmental enrichment exacerbates amyloid plaque formation in a transgenic mouse model of Alzheimer disease. J. Neuropathol. Exp. Neurol. *62*, 1220–1227.

Ji, Y., Permanne, B., Sigurdsson, E.M., Holtzman, D.M., and Wisniewski, T. (2001). Amyloid beta40/42 clearance across the blood-brain barrier following intra-ventricular injections in wild-type, apoE knock-out and human apoE3 or E4 expressing transgenic mice. J. Alzheimers Dis. *3*, 23–30.

Kamenetz, F., Tomita, T., Hsieh, H., Seabrook, G., Borchelt, D., Iwatsubo, T., Sisodia, S., and Malinow, R. (2003). APP processing and synaptic function. Neuron *37*, 925–937.

Kempermann, G., Kuhn, H.G., and Gage, F.H. (1997). More hippocampal neurons in adult mice living in an enriched environment. Nature *386*, 493–495.

Kempermann, G., Kuhn, H.G., and Gage, F.H. (1998). Experience-induced neurogenesis in the senescent dentate gyrus. J. Neurosci. *18*, 3206–3212.

Kim, S.H., Leem, J.Y., Lah, J.J., Slunt, H.H., Levey, A.I., Thinakaran, G., and Sisodia, S.S. (2001). Multiple effects of aspartate mutant presenilin 1 on the processing and trafficking of amyloid precursor protein. J. Biol. Chem. *276*, 43343–43350.

Kramer, A.F., Colcombe, S., Erickson, K., Belopolsky, A., McAuley, E., Cohen, N.J., Webb, A., Jerome, G.J., Marquez, D.X., and Wszalek, T.M. (2002). Effects of aerobic fitness training on human cortical function: a proposal. J. Mol. Neurosci. *19*, 227–231.

Lazarov, O., Lee, M., Peterson, D.A., and Sisodia, S.S. (2002). Evidence that synaptically released beta-amyloid accumulates as extracellular deposits in the hippocampus of transgenic mice. J. Neurosci. *22*, 9785–9793.

Lee, E.H., Hsu, W.L., Ma, Y.L., Lee, P.J., and Chao, C.C. (2003). Enrichment enhances the expression of sgk, a glucocorticoid-induced gene, and facilitates spatial learning through glutamate AMPA receptor mediation. Eur. J. Neurosci. *18*, 2842–2852.

Li, C., and Hersh, L.B. (1995). Neprilysin: assay methods, purification, and characterization. Methods Enzymol. *248*, 253–263.

Marr, R.A., Rockenstein, E., Mukherjee, A., Kindy, M.S., Hersh, L.B., Gage, F.H., Verma, I.M., and Masliah, E. (2003). Neprilysin gene transfer reduces human amyloid pathology in transgenic mice. J. Neurosci. *23*, 1992–1996.

Mattson, M.P. (2000). Neuroprotective signaling and the aging brain: take away my food and let me run. Brain Res. *886*, 47–53.

Mattson, M.P., Duan, W., Lee, J., and Guo, Z. (2001). Suppression of brain aging and neurodegenerative disorders by dietary restriction and environmental enrichment: molecular mechanisms. Mech. Ageing Dev. *122*, 757–778.

Mechtcheriakova, D., Wlachos, A., Holzmuller, H., Binder, B.R., and Hofer, E. (1999). Vascular endothelial cell growth factor-induced tissue factor expression in endothelial cells is mediated by EGR-1. Blood *93*, 3811–3823.

Miller, B.C., Eckman, E.A., Sambamurti, K., Dobbs, N., Chow, K.M., Eckman, C.B., Hersh, L.B., and Thiele, D.L. (2003). Amyloid-beta peptide levels in brain are inversely correlated with insulysin activity levels in vivo. Proc. Natl. Acad. Sci. USA *100*, 6221–6226.

Nitsch, R.M., Farber, S.A., Growdon, J.H., and Wurtman, R.J. (1993). Release of amyloid beta-protein precursor derivatives by electrical depolarization of rat hippocampal slices. Proc. Natl. Acad. Sci. USA *90*, 5191–5193.

Pinsky, D.J., Broekman, M.J., Peschon, J.J., Stocking, K.L., Fujita, T., Ramasamy, R., Connolly, E.S., Jr., Huang, J., Kiss, S., Zhang, Y., et al. (2002). Elucidation of the thromboregulatory role of CD39/ectoapyrase in the ischemic brain. J. Clin. Invest. *109*, 1031–1040.

Price, D.L., and Sisodia, S.S. (1998). Mutant genes in familial Alzheimer's disease and transgenic models. Annu. Rev. Neurosci. *21*, 479–505.

Rampon, C., Tang, Y.P., Goodhouse, J., Shimizu, E., Kyin, M., and Tsien, J.Z. (2000). Enrichment induces structural changes and recovery from nonspatial memory deficits in CA1 NMDAR1-knockout mice. Nat. Neurosci. *3*, 238–244.

Sapolsky, R.M. (1993). The physiology of dominance in stable versus unstable social hierarchies. In Primate Social Conflict, W. Mason and S. Mendoza, eds. (New York: SUNY Press), pp. 171.

SenBanerjee, S., Lin, Z., Atkins, G.B., Greif, D.M., Rao, R.M., Kumar, A., Feinberg, M.W., Chen, Z., Simon, D.I., Luscinskas, F.W., et al. (2004). KLF2 is a novel transcriptional regulator of endothelial proinflammatory activation. J. Exp. Med. *199*, 1305–1315.

Seo, J., Bakay, M., Chen, Y.W., Hilmer, S., Shneiderman, B., and Hoffman, E.P. (2004). Interactively optimizing signal-to-noise ratios in expression profiling: project-specific algorithm selection and detection p-value weighting in Affymetrix microarrays. Bioinformatics *20*, 2534–2544.

Seubert, P., Vigo-Pelfrey, C., Esch, F., Lee, M., Dovey, H., Davis, D., Sinha, S., Schlossmacher, M., Whaley, J., Swindlehurst, C., et al. (1992). Isolation and quantification of soluble Alzheimer's beta-peptide from biological fluids. Nature *359*, 325–327.

Shibata, M., Yamada, S., Kumar, S.R., Calero, M., Bading, J., Frangione, B., Holtzman, D.M., Miller, C.A., Strickland, D.K., Ghiso, J., and Zlokovic, B.V. (2000). Clearance of Alzheimer's amyloid-ss(1–40) peptide from brain by LDL receptor-related protein-1 at the blood-brain barrier. J. Clin. Invest. *106*, 1489–1499.

Silverman, E.S., and Collins, T. (1999). Pathways of Egr-1-mediated gene transcription in vascular biology. Am. J. Pathol. *154*, 665–670.

Sisodia, S.S., Koo, E.H., Hoffman, P.N., Perry, G., and Price, D.L. (1993). Identification and transport of full-length amyloid precursor proteins in rat peripheral nervous system. J. Neurosci. *13*, 3136–3142.

Song, E.S., Juliano, M.A., Juliano, L., and Hersh, L.B. (2003). Substrate activation of insulin-degrading enzyme (insulysin). A potential target for drug development. J. Biol. Chem. *278*, 49789–49794.

Stein, T.D., and Johnson, J.A. (2002). Lack of neurodegeneration in transgenic mice overexpressing mutant amyloid precursor protein is associated with increased levels of transthyretin and the activation of cell survival pathways. J. Neurosci. *22*, 7380–7388.

Suzuki, N., Cheung, T.T., Cai, X.D., Odaka, A., Otvos, L., Jr., Eckman, C., Golde, T.E., and Younkin, S.G. (1994). An increased percentage of long amyloid beta protein secreted by familial amyloid beta protein precursor (beta APP717) mutants. Science *264*, 1336–1340.

Swain, R.A., Harris, A.B., Wiener, E.C., Dutka, M.V., Morris, H.D., Theien, B.E., Konda, S., Engberg, K., Lauterbur, P.C., and Greenough, W.T. (2003). Prolonged exercise induces angiogenesis and increases cerebral blood volume in primary motor cortex of the rat. Neuroscience *117*, 1037–1046.

Tong, L., Shen, H., Perreau, V.M., Balazs, R., and Cotman, C.W. (2001). Effects of exercise on gene-expression profile in the rat hippocampus. Neurobiol. Dis. *8*, 1046–1056.

Tsai, K.J., Chen, S.K., Ma, Y.L., Hsu, W.L., and Lee, E.H. (2002). sgk, a primary glucocorticoid-induced gene, facilitates memory consolidation of spatial learning in rats. Proc. Natl. Acad. Sci. USA *99*, 3990–3995.

Turner, R.S., Suzuki, N., Chyung, A.S., Younkin, S.G., and Lee, V.M. (1996). Amyloids beta40 and beta42 are generated intracellularly in cultured human neurons and their secretion increases with maturation. J. Biol. Chem. *271*, 8966–8970.

Turner, A.J., Isaac, R.E., and Coates, D. (2001). The neprilysin (NEP) family of zinc metalloendopeptidases: genomics and function. Bioessays *23*, 261–269.

Urade, Y., and Hayaishi, O. (2000). Biochemical, structural, genetic, physiological, and pathophysiological features of lipocalin-type prostaglandin D synthase. Biochim. Biophys. Acta *1482*, 259–271.

van Praag, H., Kempermann, G., and Gage, F.H. (1999). Running increases cell proliferation and neurogenesis in the adult mouse dentate gyrus. Nat. Neurosci. *2*, 266–270.

van Praag, H., Kempermann, G., and Gage, F.H. (2000). Neural consequences of environmental enrichment. Nat. Rev. Neurosci. *1*, 191–198.

Wang, J., Tanila, H., Puolivali, J., Kadish, I., and Groen, T. (2003). Gender differences in the amount and deposition of amyloidbeta in APPswe and PS1 double transgenic mice. Neurobiol. Dis. *14*, 318–327.

Weidemann, A., Konig, G., Bunke, D., Fischer, P., Salbaum, J.M., Masters, C.L., and Beyreuther, K. (1989). Identification, biogenesis, and localization of precursors of Alzheimer's disease A4 amyloid protein. Cell *57*, 115–126.

Yasojima, K., Akiyama, H., McGeer, E.G., and McGeer, P.L. (2001a). Reduced neprilysin in high plaque areas of Alzheimer brain: a possible relationship to deficient degradation of beta-amyloid peptide. Neurosci. Lett. *297*, 97–100.

Yasojima, K., McGeer, E.G., and McGeer, P.L. (2001b). Relationship between beta amyloid peptide generating molecules and neprilysin in Alzheimer disease and normal brain. Brain Res. *919*, 115–121.